

# Differentiable and Transportable Structure Learning

**Jeroen Berrevoets**  
 University of Cambridge  
 jb2384@cam.ac.uk

**Nabeel Seedat**  
 University of Cambridge  
 ns741@cam.ac.uk

**Fergus Imrie**  
 UCLA  
 imrie@ucla.edu

**Mihaela van der Schaar**  
 University of Cambridge,  
 UCLA, Alan Turing Institute  
 mv472@cam.ac.uk

## Abstract

We are interested in unsupervised structure learning with a particular focus on directed acyclic graphical (DAG) models. Compute required to infer these structures is typically super-exponential in the amount of variables, as inference requires a sweep of a combinatorially large space of potential structures. That is, until recent advances allowed to search this space using a differentiable metric, drastically reducing search time. While this technique—named NOTEARS—is widely considered a seminal work in DAG-discovery, it concedes an important property in favour of differentiability: *transportability*. In our paper we introduce *D-Struct* which recovers transportability in the found structures through a novel architecture and loss function, while remaining completely differentiable. As D-Struct remains differentiable, one can easily adopt our method in differentiable architectures as was previously done with NOTEARS. In our experiments we empirically validate D-Struct with respect to edge accuracy and the structural Hamming distance.

## 1 Introduction

Machine learning has proven to be a crucial tool in many disciplines. With successes in medicine [1–5], economics [6–8], physics [9–14], robotics [15–18], and even entertainment [19–21], machine learning is transforming the way in which experts interact with their field. These successes are in large part due to increasing accuracy of diagnoses, marketing campaigns, analyses of experiments, and so forth. However, we believe that machine learning has much more to offer than improved accuracy. In fact, recent advances seem to back up this claim, as machine learning is slowly recognised as a tool for scientific discovery [22–25]. These successes are the result of cases where machine learning suggests a relationship between variables. Discovering such relationships are the focus of our paper as we aim to aid discovery through differentiable *and* transportable structure learning.

**The structures.** We focus on discovering directed acyclic graphs (DAG) in a domain  $\mathcal{X}$ . Such a DAG helps us to understand how different variables in  $\mathcal{X}$  interact with each other. Consider a three-variable domain  $\mathcal{X} := \{X, Y, Z\}$ , governed by a joint-distribution,  $\mathbb{P}_{\mathcal{X}}$ . Estimating  $\mathbb{P}_{\mathcal{X}}$  may be enough in some settings, but it gives us no information regarding specific interactions in  $\mathcal{X}$ . In contrast, consider the following:  $\mathcal{G} = (X \rightarrow Z \rightarrow Y)$ , where  $\mathcal{G}$  depicts  $\mathbb{P}_{\mathcal{X}}$  as a DAG.  $\mathcal{G}$  still depicts  $\mathbb{P}_{\mathcal{X}}$  [26], but with more to deduce [27]. For example, we learn that  $X$  does not directly influence  $Y$ . We also learn that  $X \perp\!\!\!\perp Y | Z$ , as  $X$  does not give us any additional information on  $Y$  once we know  $Z$ . This is due to d-separation, introduced formally in section 2.

The latter forms the basis for conventional DAG-structure learning [28]. In particular, with  $X \perp\!\!\!\perp Y | Z$  we strongly limit the potential DAGs. Given more variables (and more independence statements), we

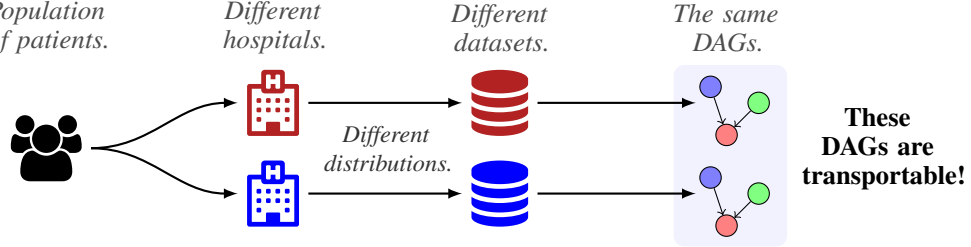


Figure 1: **Transportability in scientific discovery.** Different patients go to different hospitals (left), yet we wish to infer a *general* structure (right) *across* hospitals. A structure can only be considered a discovery if it generalizes across distributions over the same domain. For example, the way blood pressure interacts with heart disease is the same for all humans and should be reflected in the structure.

limit the potential DAGs further. However, independence tests are computationally expensive which is problematic as the amount of potential DAGs increases super-exponentially in  $|\mathcal{X}|$  [29].

This limitation strongly impacted adoption of DAG-learning, until Zheng et al. [30] proposed NOTEARS— a differentiable metric to evaluate whether or not a discovered structure is a DAG [30, 31]. Relying on the advances of automatic differentiation, NOTEARS learns a DAG-structure in a much more efficient way than earlier methods based on conditional independence tests (CITs).

Clearly, NOTEARS is the way forward from CIT-based methods. However, we recognise a limitation: a found DAG does not generalise to equally factorisable distributions, i.e. NOTEARS is not *transportable*. While we why this is the case in section 2.2 (and confirm it empirically in section 4), we give a brief description of the problem below, helping us to clearly state our contribution.

**Transportability.** Consider fig. 1 which depicts two hospitals: and , named hospitals A and B onward. Each hospital hosts patients, which are described by the same set of features such as age, gender, blood-group, etc. However, the hospitals may differ in terms of their patient-distribution, e.g. A hosts more elderly people compared to B. If we use NOTEARS to learn a DAG from data on hospital A, we have actually no guarantee that the same DAG is discovered from data in hospital B.

Interestingly, despite computational limitations, transportability is actually guaranteed when using a CIT-based discovery method [32, 33], assuming that patients in both hospitals exhibit the same (in)dependencies in their covariates. Having no guarantee to transport findings across distributions is a major shortcoming, as replicating a found discovery is considered a hallmark of the scientific method [34–37]. We extend NOTEARS by enforcing transportability, while still remaining differentiable.

**Contribution.** In this paper, we present *D-Struct*. D-Struct is the first *transportable* differential structure learner. Being transportable grants D-Struct several advantages over the state-of-the art: D-Struct is more robust, even when in the conventional single-dataset case; D-Struct is fast, in fact, we report time-to-convergence often up to 20 times faster than NOTEARS and other DSFs; and given its completely differentiable architecture, D-Struct can easily be incorporated in existing differentiable frameworks such as is the case with other differentiable structure learners (e.g. [38–42]).

While transportable methods have clear benefits over non-transportable methods in settings with multiple datasets (as is illustrated in our example in fig. 1), we emphasise that our method is not limited to these settings alone. In fact, we find that enforcing transportability significantly increases performance in settings with one dataset, which is arguably most common. In section 3.2 we explain how to use our ideas in the single dataset setting, which we empirically validate in section 4.

## 2 Preliminaries and related work

We aim to build a transportable in differentiable structure learner, with a specific focus on directed acyclic graphs (DAGs). With NOTEARS [30] (and refinements [31, 43–45]) as the most adopted method to learn DAGs through continuous optimisation we focus our discussion mostly on NOTEARS, without loss of generality. However, first we introduce our definition of transportability, and then explain how NOTEARS works and why it is not transportable. We will also explain that our observation generalises to other continuous optimisation techniques for DAG-discovery.

## 2.1 Transportability

**Factorisation and independence.** Consider a distribution,  $\mathbb{P}_{\mathcal{X}}$ , which we can factorise into,

$$\prod_i \mathbb{P}_{\mathcal{X}_i | \mathcal{X}_{i+1:d}}, \quad (1)$$

with  $i \in [d]$ , where  $[d] := 1, \dots, d$ , and  $\mathcal{X}_i$  representing the  $i^{\text{th}}$  element in  $\mathcal{X}$ . Depending on  $d$ , eq. (1), may get quite long as in the worst case the conditions contain  $d - 1$  different variables. The latter may become restrictive when estimating and decomposing  $\hat{\mathbb{P}}_{\mathcal{X}}$  from data, especially in large  $d$ . Instead, one may wish to simplify eq. (1), using independence statements. For example,  $\mathcal{X}_i \perp\!\!\!\perp \mathcal{X}_k$  invokes following simplification:  $\mathbb{P}_{\mathcal{X}_i | \mathcal{X}_{j,k}} = \mathbb{P}_{\mathcal{X}_i | \mathcal{X}_j}$ . Having a simplified version of eq. (1), translates into a smaller *Markov blanket* and *Markov boundary* [46] (see appendix D for more details).

**Non-symmetrical statements.** In this paper we are interested in *directed* structures, i.e. rather than only relating variables in a symmetric sense (as is the case for independence statements above), we wish to infer parent and child relationships. A collection of such relationships is named a *directed acyclic graph* (DAG), denoted  $\mathcal{G}_{\mathcal{X}} := \{\mathcal{X}, \mathcal{E}\}$ , where  $\mathcal{E} \subset \mathcal{X} \times \mathcal{X}$  is a set of edges connecting nodes (corresponding to random variables) in  $\mathcal{X}$ , with  $(\mathcal{X}_i, \mathcal{X}_j) \in \mathcal{E} \neq (\mathcal{X}_j, \mathcal{X}_i)$  indicating a direction [47].

Despite independence being symmetric, it is still possible to infer non-symmetric relationships with only independence statements through d-separation [48–53]. Given a collection of conditional independence statements, which renders two variables independent given a third:  $X \perp\!\!\!\perp Y | Z$ , d-separation in def. 1 helps us narrow down a directed structure from independence statements [54, 55]<sup>1</sup>.

**Definition 1** (d-separation [29]). *In a DAG  $\mathcal{G}$ , a path between nodes  $\mathcal{X}_i$  and  $\mathcal{X}_j$  is blocked by a set  $\mathcal{X}_d \subset \mathcal{X}$  (which excludes  $\mathcal{X}_i$  and  $\mathcal{X}_j$ ) whenever there is a node  $\mathcal{X}_k$ , such that one of the following two possibilities holds:*

(1)  $\mathcal{X}_k \in \mathcal{X}_d$  and

$$\begin{aligned} & \mathcal{X}_{k-1} \leftarrow \mathcal{X}_k \leftarrow \mathcal{X}_{k+1}, \\ \text{or} \quad & \mathcal{X}_{k-1} \rightarrow \mathcal{X}_k \rightarrow \mathcal{X}_{k+1}, \\ \text{or} \quad & \mathcal{X}_{k-1} \leftarrow \mathcal{X}_k \rightarrow \mathcal{X}_{k+1}. \end{aligned}$$

(2) neither  $\mathcal{X}_k$  nor any of its descendants is in  $\mathcal{X}_d$  and

$$\mathcal{X}_{k-1} \rightarrow \mathcal{X}_k \leftarrow \mathcal{X}_{k+1}.$$

Furthermore, in a DAG  $\mathcal{G}$ , we say that two disjoint subsets  $\mathcal{A}$  and  $\mathcal{B}$  are d-separated by a third (also disjoint) subset  $\mathcal{X}_d$  if every path between nodes in  $\mathcal{A}$  and  $\mathcal{B}$  is blocked by  $\mathcal{X}_d$ . We then write

$$\mathcal{A} \perp\!\!\!\perp \mathcal{B} | \mathcal{X}_d.$$

When  $\mathcal{X}_d$  d-separates  $\mathcal{A}$  and  $\mathcal{B}$  in  $\mathcal{G}$ , we will denote this as  $d\text{-sep}_{\mathcal{G}}(\mathcal{A}; \mathcal{B} | \mathcal{X}_d)$ .

With d-separation in def. 1, we have a *back-and-forth* relationship between a DAG-structure  $\mathcal{G}_{\mathcal{X}}$ , and the distribution  $\mathbb{P}_{\mathcal{X}}$ . Specifically, the conditional independence relationships defined in  $\mathcal{G}_{\mathcal{X}}$  should have a one-to-one correspondence with those found in  $\mathbb{P}_{\mathcal{X}}$  [56], i.e. if  $X \perp\!\!\!\perp Y | Z$  then  $X \perp\!\!\!\perp \mathcal{Y} | \mathcal{Z}$ , where  $\perp\!\!\!\perp_{\mathcal{S}}$  denotes independence in  $\mathcal{S}$ .

The set of conditional independence assertions in  $\mathbb{P}$  is denoted as  $\mathcal{I}(\mathbb{P})$ . Similarly, all independence statements implied by d-separation in a graph  $\mathcal{G}$  are denoted as  $\mathcal{I}(\mathcal{G}) = \{(\mathcal{X} \perp\!\!\!\perp \mathcal{B} | \mathcal{X}_d) : d\text{-sep}_{\mathcal{G}}(\mathcal{A}; \mathcal{B} | \mathcal{X}_d)\}$ , referred to as the set of *global Markov independencies* [26, Chapter 3].

**Invariance and discovery.** Consider two datasets:  $\mathcal{D}_1 = \{X^{(n)} \in \mathcal{X} : n \in [N]\}$  and  $\mathcal{D}_2 = \{X^{(m)} \in \mathcal{X} : m \in [M]\}$ , spanning the same space  $\mathcal{X}$ . As a sample  $X^{(n)}$  from  $\mathcal{D}_1$  depicts the same variables as a sample  $X^{(m)}$  from  $\mathcal{D}_2$ , both datasets reflect the *same* underlying mechanisms such as smoking and its effect on cancer.

Of course, while the samples in  $\mathcal{D}_1$  and  $\mathcal{D}_2$  come from the same domain  $\mathcal{X}$ , they may be sampled from different distributions,  $\mathbb{P}_{\mathcal{X}}^1$  and  $\mathbb{P}_{\mathcal{X}}^2$ , respectively. Recall fig. 1, where hospitals A and B may be

<sup>1</sup>Note that in these earlier works DAGs were named *influence diagrams*.

located in different regions, resulting in the type of patient they host to also be different. However, key in a scientific discovery is that it generalises *beyond* distributions and is carried over through the entire domain  $\mathcal{X}$ . In other words, any structure we may find in  $\mathcal{D}_1$ , should also be found in  $\mathcal{D}_2$ , as for almost all distributions  $\mathbb{P}_{\mathcal{X}}^i \in \mathcal{P}$  that factorise over  $\mathcal{G}^2$  we have that  $\mathcal{I}(\mathbb{P}_{\mathcal{X}}^i) = \mathcal{I}(\mathcal{G}) = \mathcal{I}(\mathbb{P}_{\mathcal{X}}^j)$  where  $\mathbb{P}_{\mathcal{X}}^i \neq \mathbb{P}_{\mathcal{X}}^j$  [26, Theorem 3.5], otherwise we haven't discovered anything at all.

**Definition 2** (Transportability). *With multiple datasets,  $\{\mathcal{D}_k \sim \mathbb{P}_{\mathcal{X}}^k : k \in [K]\}$  over the same domain  $\mathcal{X}$ , sampled from potentially different distributions  $\mathbb{P}_{\mathcal{X}}^i \neq \mathbb{P}_{\mathcal{X}}^j$  if  $i \neq j$  for all  $i, j \in [K]$ , we call a method *transportable* if it learns a structure that is the same across all distributions:  $\{\mathcal{D}_k \rightarrow \mathcal{G}_k : k \in [K]\}$  s.t.  $\mathcal{G}_1 = \dots = \mathcal{G}_K$ .*

Def. 2 states that when a DAG found in  $\mathcal{D}_1$  is also found in  $\mathcal{D}_2$ , we consider that DAG, and the method proposing it, *transportable*. Transportability in CIT-based methods is only satisfied when we assume that each distribution contains the same global Markov independencies. This assumption is not strict at all, as we are only concerned with distributions that span the same domain  $\mathcal{X}$ , and thus inherit the same interactions as posed by  $\mathcal{X}$ , i.e. the discoveries to be made. As such, CIT-based methods learn transportable DAGs automatically as transportability is a property directly related to the set of independencies of both distributions and DAGs, which we assume to be the same.

From the above, it is clear that transportability is a property of the structure learning method itself. In the case of CIT-based methods, we are guaranteed transportability in our setting, but not so for differentiable structure learnings. However, given that the method is responsible for transportability, we can come up with ways to include this property in differentiable structure learners also.

## 2.2 Differentiable structure learning

**Shortcomings of CIT-based methods.** Using  $\mathcal{I}(\mathbb{P})$ , CIT-based methods will evaluate each graph depicted over  $\mathcal{X}$  with respect to its factorisation as per  $\mathcal{I}(\mathcal{G} \in \mathbb{G}_{\mathcal{X}})$ , where  $\mathbb{G}_{\mathcal{X}}$  denotes the space of all possible DAGs in the domain  $\mathcal{X}$ . Based on  $\mathcal{I}(\mathcal{G})$  one can devise a score, which is used to select the DAGs that do not violate the factorisation posed by  $\mathcal{I}(\mathbb{P})$ , which is composed using conditional independence tests. The above results in a set of potential DAGs. Further iterations on CIT-based methods are then focused on reducing this set as much as possible, usually in function of some additional parametric assumptions on the functional classes in the structural equations of the sought after DAG, yet the overarching goal of equating  $\mathcal{I}(\mathbb{P})$  and  $\mathcal{I}(\mathcal{G})$  remains constant throughout methods.

The major issue with the above is computation. CIT-based methods take too long—especially with larger  $\mathcal{X}$ . Essentially, there are two aspects which negatively impact computation time: firstly, the amount of potential DAGs (all of which need to be scored) increases super-exponentially in  $|\mathcal{X}|$  [29]; and secondly, the score itself is not differentiable with respect to the evaluated DAG, i.e., we cannot traverse  $\mathbb{G}_{\mathcal{X}}$  in a smart way based on the score of DAGs that are already evaluated.

**Differentiable score functions.** Enter *differentiable* score functions (DSFs). With DSFs one *can* traverse  $\mathbb{G}_{\mathcal{X}}$  smartly to arrive at a DAG much faster. Furthermore, with a differentiable method, it is straightforward to include them in a variety of different differentiable architectures as well, allowing joint optimisation of both the graphical structure as well as the accompanying structural equations.

Most notable is NOTEARS [30, 31], which proposes following objective:

$$\min_{A \in \mathcal{A}} F(A) + \lambda_1 \|A\|_1 + \frac{\rho}{2} |h(A)|^2 + \lambda_2 h(A), \quad (2)$$

where  $A \in \{0, 1\}^{d \times d}$  denotes an adjacency matrix (corresponding to  $\mathcal{E}$  in  $\mathcal{G}$ ), and  $F(A)$  is a likelihood based loss (such as the mean squared error),  $\rho$  and  $\lambda_{1,2}$  are scalar hyperparameters, and

$$h(A) := \text{tr}(\exp(A \circ A)) - d, \quad (3)$$

is the actual differentiable score function, where  $\text{tr}(\cdot)$  is the matrix trace operator, and  $\circ$  is the element-wise (Hadamard) product. Importantly,  $h(A) = 0$  indicates  $A$  to be a DAG. Considering that eq. (3) is differentiable, we can take its derivative with respect to  $A$  and minimise eqs. (2) and (3) through  $A$ .

While other DSFs exist [44, 45], the idea is the same. Essentially, one randomly initialises  $A$  and optimises a loss which includes the DSF, such as  $h(A)$ . As the optimisation procedure is always based

---

<sup>2</sup>For all distributions except for a set of measure zero in the space of conditional probability distribution parameterizations [32]

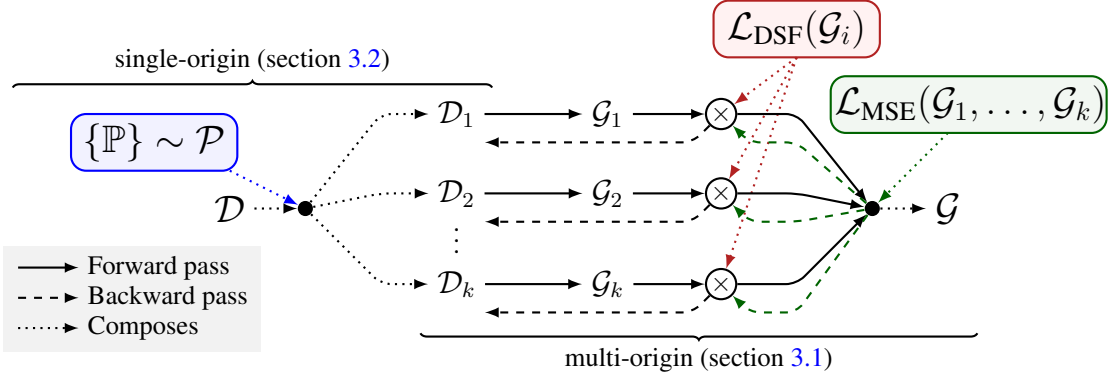


Figure 2: **D-Struct architecture.** Above architecture enforces transportability. The architecture is split in two major parts: single-origin (discussed in section 3.2) and multi-origin (discussed in section 3.1). There are three components:  $\mathcal{P}$ ,  $\mathcal{L}_{\text{DSF}}$ , and  $\mathcal{L}_{\text{MSE}}$ . Each component is combined and backpropagated through the architecture. After training, each DSF “votes” for the final structure  $\mathcal{G}$ .

on a previous evaluation (as is always the case for gradient-based learning), the random initialisation of  $A$  may guide the optimisation in different directions, potentially arriving at a local minimum in the case of non-convex targets. The latter is certainly the case in more recent improvements of NOTEARS as they almost exclusively focus on non-linear structural equations.

**Transportability of DSFs.** DSFs are not transportable. The reason is mainly due to eqs. (2) and (3) having multiple solutions, compared to the single solution that transforms  $\mathcal{I}(\mathbb{P})$  to  $\mathcal{G}^3$ . Similar observations can be made with other DSFs as well. In essence, the approximate nature of (stochastic) gradient-based learning can result in conflicting estimate structures given different datasets.

### 3 D-Struct: Differentiable and transportable structure learning

The goal of any gradient-based structure learner is to transform data into a structure:

$$\mathcal{D} \rightarrow \mathcal{G},$$

and so is the case for D-Struct. However, we consider D-Struct to be a general framework, just as transportability is a general problem for all contemporary DSFs (due to the nature of gradient-based optimisation). As such, we first introduce D-Struct generally in section 3.1 and provide an example implementation for NOTEARS in section 3.3. In section 3.2, we explain how one can solve for transportability in the setting where there is only one dataset. Recall from section 1 and def. 2 that transportability is an artifact of there existing more than one dataset, however, we show (in section 4) that even with a “single-origin” dataset, D-Struct offers more accurate DAGs.

#### 3.1 General algorithm

In order to enforce transportability, D-Struct employs an ensemble-architecture of multiple initialisations of the chosen DSF and their appropriate (differentiable) architecture, combined with a regularisation function based on the D-Struct architecture. Consider fig. 2 where we depict this architecture and highlight how the regularisation is backpropagated throughout the entire network.

Given distinct datasets  $\mathcal{D}_1, \dots, \mathcal{D}_K$ , we can use any DSF (e.g. [30, 31, 43–45]) to learn a graphical structure. Specifically, we let  $K$  *distinct* DSFs learn a DAG from one of the  $K$  datasets, agnostic from each other. We consider these learning objectives to be  $K$  parallel objectives, as is also illustrated in fig. 2 in the rightmost part (annotated with “multi-origin”). Crucially, D-Struct does not restrict which type of DSF we should use. For example, in a linear setting one can use vanilla NOTEARS, whereas in a non-linear setting, one could simply use the non-parametric NOTEARS-Sob or NOTEARS-MLP. Naturally, any restriction posed by the chosen DSL will carryover to D-Struct. While we focus on NOTEARS-MLP in our main text (cfr. our experiments in section 4), appendix A also includes results of D-Struct paired with other DSFs.

At this point, we identify a first loss term:  $\mathcal{L}_{\text{DSF}}(\mathcal{G}_k)$ , which depends on the chosen DSF (illustrated in red in fig. 2). For example, NOTEARS will evaluate the structure  $\mathcal{G}_k$  using eqs. (3) and (4). Whenever data is put through the architecture (recall, data stems from distinct datasets and cannot be mixed), we

<sup>3</sup>With one method that is, different CIT-based methods will yield different graphs also. Recall from def. 2 that transportability is a property of a method.

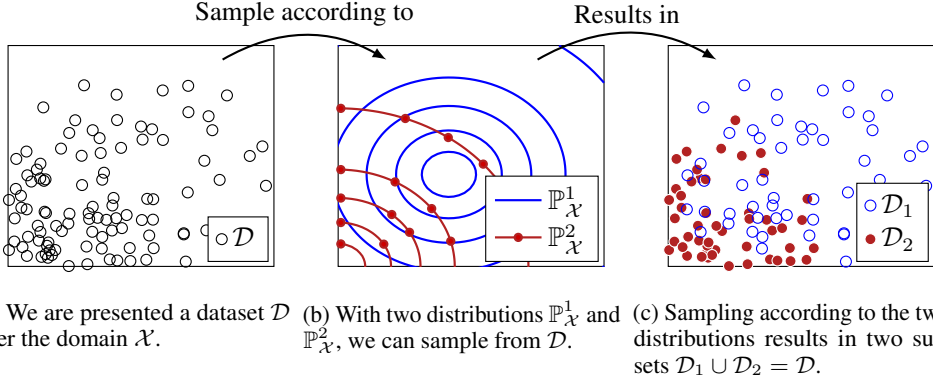


Figure 3: **Differently distributed single-origin data.** On the left we illustrate a single-origin dataset  $\mathcal{D}$ , sampled from one distribution. In the middle we illustrate two distributions over the domain of  $\mathcal{D}$ , which are used to resample two subsets from  $\mathcal{D}$ , thereby creating a *synthetic* multi-origin datasource.

evaluate the found structure with respect to the relevant data as  $\mathcal{L}_{\text{DSF}}(\mathcal{G}_k | \mathbf{X} \sim \mathcal{D}_k)$ , where  $\mathbf{X} \subseteq \mathcal{D}$ . Note that, if the chosen DSF requires hyperparameters (such as  $\lambda_{1,2}$  and  $\rho$  in eq. (4)), we have to include these in the set of required hyperparameters of D-Struct. While it is possible to set different hyperparameter values for each of the DSFs (possibly helpful when there is a lot of variety across datasets), we fix these across DSFs in light of simplicity but give an overview in appendix A.1.

Given  $\{\mathcal{L}_{\text{DSF}}(\mathcal{G}_k) : k \in [K]\}$  we can enforce transportability across  $\mathcal{D}_k$  by comparing the structures  $\mathcal{G}_1, \dots, \mathcal{G}_k$ . We do this by calculating the difference of the adjacency matrices  $A_k \in \{0, 1\}^{d \times d}$ . Specifically, for each gradient calculation (before we perform a backward pass), we take the mean adjacency matrix,  $\bar{A}(A_1, \dots, A_K) = \frac{1}{K} \sum_k A_k$ , detach it from the gradient and backpropagate the mean squared error for each parallel DSF. Doing this results in the following regularisation term:

$$\mathcal{L}_{\text{MSE}}(A_k) := \|A_k - \bar{A}(A_1, \dots, A_K)\|_2^2, \quad (4)$$

which is added to the DSF loss as follows (and illustrated in green in fig. 2),

$$\mathcal{L}(\mathcal{G}_k | \mathcal{D}_k) := \mathcal{L}_{\text{DSF}}(\mathcal{G} | \mathcal{D}_k) + \alpha \mathcal{L}_{\text{MSE}}(A(\mathcal{G}_k)), \quad (5)$$

where  $A(\mathcal{G})$  indicates the adjacency matrix of  $\mathcal{G}$ , and  $\alpha$  is a scalar hyperparameter (refer to appendix A.1 for hyperparameter settings, details, and further insights). Note that the second term in eq. (5) does not depend on  $\mathcal{D}_k$ . Having  $\mathcal{L}_{\text{MSE}}$  be agnostic to the data makes sense as transportability is not a property of the data. Indeed, recall from section 2.1 that transportability is a property of the structure learner instead. Having this additional term (based solely on the parallel learners) enforces transportability as the architecture encourages the DSFs to converge to the same DAG.

### 3.2 Transportability in a single-origin dataset

So far, we have only discussed the rightmost part in fig. 2, annotated by ‘‘multi-origin’’. In section 3.1 we assumed data is provided in multiple distinct datasets, i.e. they stem from a multi-origin datasource. However, here we explain how even in the single-origin case D-Struct is applicable, irrespective of which DSF we end up choosing. As such, we continue our discussion by explaining the leftmost part of fig. 2, annotated by ‘‘single origin’’.

While a multi-origin datasource may be governed by multiple distributions, a single-origin one is not. Our task is clear: from a single-origin datasource, we have to *mimic* a multi-origin datasource in such a way that we know each subset has a different distribution, yet maintains the original properties of the single-origin-distribution (such as the global Markov independencies). Doing so allows us to enforce def. 2 through the architecture in fig. 2.

In fig. 2 we show that we handle the single-origin case by transforming it to a multi-origin case. With this *synthetic* multi-origin setup, we can continue using

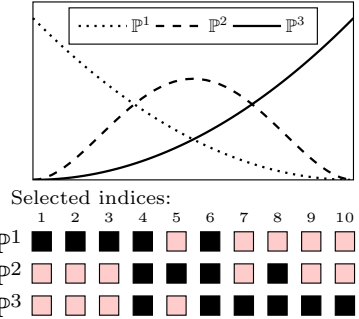


Figure 4:  **$K$  distributions.** We have illustrated the subset sampling with beta-distributions above, for  $K = 3$ . For each density, we evaluate its PDF for each index, normalize it and perform a Bernoulli experiment. The selected indices are plotted below the density functions (black indicates a selected index).

D-Struct as we have done in section 3.1. More specifically, we preface the multi-origin case by a step that divides  $\mathcal{D}$  into subsets  $\{\mathcal{D}_1, \dots, \mathcal{D}_k\}$ , according to different distributions  $\mathcal{P} := \{\mathbb{P}_{\mathcal{X}}^1, \dots, \mathbb{P}_{\mathcal{X}}^k\}$ . Consider fig. 3 where we illustrate how one may apply an *alternative* distribution to  $\mathbb{P}_{\mathcal{X}}$  which governs  $\mathcal{D}$ . In principle, each element  $X^{(n)} \in \mathcal{D}$  has a  $\mathcal{P}_k(X^{(n)})$  probability to be sampled from  $\mathcal{D}$ . As such, each distribution leads to a subset  $\mathbb{P}_k \times \mathcal{D} \rightarrow \mathcal{D}_k$  where  $\bigcup_k \mathcal{D}_k = \mathcal{D}$ , and  $\mathcal{D}_k$  need not be disjoint but cannot contain  $\mathcal{D}$  completely.

In our experiments we perform this preprocessing step by first correlating the index of each element in  $\mathcal{D}$  with their values in  $\mathcal{X}$ . Next, we define  $K$  distributions over  $[N]$  and sample indices accordingly. The sampled indices compose the subset. Below we explain each component in detail.

◆ *Correlating indices and values.* Sorting and reindexing elements in  $\mathcal{D}$  according to the covariates in  $\mathcal{X}$  ensures a dependency between  $\mathcal{X}$  and  $i \in [N]$ , where  $i < j$  indicates  $X^{(i)} < X^{(j)}$ , i.e. the *order* of  $X$ 's in the data structure representing  $\mathcal{D}$  is correlated with the *values* of the  $X$ 's.

◆ *Distributions over  $[N]$ .* This dependency allows us to create subsets based on one-dimensional distributions  $\{\mathbb{P}_{[N]}^k : k \in [K]\}$ , rather than much more complicated distributions over  $\mathcal{X}$ . An added bonus to these one-dimensional distributions is that they easily scale to more dimensions in  $\mathcal{X}$ . Of course, the amount of distributions, and consequentially their shape should change in function of  $K$ . Specifically, with higher  $K$ , we have to ensure that the probability mass of each distribution is concentrated in different areas of  $[K]$ . As such, we chose to model these as beta-distributions with,

$$\alpha, \beta \in \{(i, K), (K, K), (K, j) : i \in \text{interp}(1, K), j \in \text{interp}(K, 1)\},$$

where  $\text{interp}(a, b)$  is a linear interpolation between  $a$  and  $b$ , used to sample  $\lfloor \frac{K}{2} \rfloor$   $i$ 's and  $j$ 's. When  $K$  is even we leave out  $(K, K)$  such that the total amount of distributions always equals  $K$ .

◆ *Selecting indices.* Our final task is to create  $K$  subsets, which due to the first step is simplified to choosing indices instead. These indices are selected based on the distributions defined in the second step. First, we evaluate each density's PDF for every index (after normalisation:  $\frac{i}{N}$ ), and normalise the output to be a value between 0 and 1. Once we have  $K$  values for each index, we perform a Bernoulli experiment where the output determines whether or not the index is selected to be part of the subset  $k \in [K]$ . This process is illustrated in fig. 4 for  $K = 3$ .

With each subset, we apply D-Struct as explained in section 3.1. In our experiments (section 4 and appendix A) we show that D-Struct greatly improves performance of non-transportable DSFs.

### 3.3 Example: NOTEARS-MLP

D-Struct works with any DSF, though it is instructive to illustrate this with an example. For this, we chose NOTEARS-MLP [31] which is a non-parametric (cfr. the structural equations) extension of the classic NOTEARS paper. The main challenge to incorporating D-Struct into NOTEARS-MLP is to integrate it into its dual ascent strategy [30] which solves the (non-convex) constrained optimisation problem in eq. (2) [43], solved with an augmented Lagrangian method [57, Chapter 5].

```

Init.:  $\theta_k$  for each  $k \in [K]$ 
Input:  $h_{\text{tol}}$ ,  $\rho_{\text{max}}$ 
Setup:  $h \leftarrow \infty$ ,  $\rho_{1, \dots, K} \leftarrow 1$ ,  $\rho \leftarrow 1$ 
for maximum amount of epochs do
  for batch  $\sim \mathcal{D}$  do
    for  $k \in [K]$  do
      training_step( $\theta_k$ , batch);
       $h \leftarrow \max_k h(A(\theta_k))$ ;
       $\rho \leftarrow \min_k \rho_k$ ;
  
```

**Algorithm 1:** Outer-loop of dual ascent procedure for D-Struct(NOTEARS-MLP)

```

Input:  $\theta_k$ , batch
while  $\rho < \rho_{\text{max}}$  do
   $l_m \leftarrow \mathcal{L}_{\text{MSE}}(\theta_1, \dots, \theta_K)$ ;
   $l_d \leftarrow \mathcal{L}_{\text{DSF}}(\text{batch})$ ;
   $\theta \leftarrow \text{L-BFGS-B.update}(l_m, l_d)$ ;
   $h' \leftarrow h(A(\theta_k))$ ;
  if  $h' > 0.25h$  then
     $\rho_k \leftarrow 10\rho_k$ ;
  else
    break;

```

**Algorithm 2:** training\_step for D-Struct(NOTEARS-MLP)

The constraint in the optimisation problem stems from, for example, knowing that the diagonal of  $A$  can only contain zeros [30, 31, 43]. NOTEARS (and its extensions), solve this problem by using the

Table 1: **Results on Erdos-Renyì (ER) graphs.** *First block:* We sample five different ER random graphs, and accompanying non-linear structural equations using an index-model. From each system we then sample a varying amount of samples, and evaluate NOTEARS-MLP with D-Struct (indicated as “✓”) and *without* D-Struct (indicated as “✗”). *Second block:* For each row we sample a new ER graph with a varying amount of connectedness ( $s$  indicates the expected amount of edges). In both cases, we report the average performance in terms of SHD, FPR, TPR, and FDR, with std in scriptsize.

metric	SHD (↓)		FPR (↓)		TPR (↑)		FDR (↓)	
D-Struct	✓	✗	✓	✗	✓	✗	✓	✗
<i>n</i>	<i>varying sample size</i>							
200	<b>3.80</b> ±0.37	4.40±0.34	<b>2.00</b> ±0.73	4.40±0.34	0.60±0.09	<b>0.62</b> ±0.04	<b>0.27</b> ±0.06	0.44±0.03
500	<b>1.40</b> ±0.16	4.40±0.33	<b>1.20</b> ±0.25	3.80±0.27	<b>0.93</b> ±0.02	0.62±0.04	<b>0.12</b> ±0.03	0.41±0.03
1000	<b>2.28</b> ±0.18	3.67±0.82	<b>1.00</b> ±0.32	2.67±0.63	0.67±0.17	<b>0.70</b> ±0.09	<b>0.11</b> ±0.03	0.32±0.08
2000	<b>2.66</b> ±0.80	3.54±0.16	<b>1.88</b> ±0.67	2.09±0.31	<b>0.81</b> ±0.11	0.75±0.03	<b>0.27</b> ±0.07	0.33±0.00
<i>s</i>	<i>varying graph connectedness</i>							
0.5d	<b>3.75</b> ±1.6	7.33±0.13	<b>0.50</b> ±0.25	1.05±0.02	0.83±0.19	<b>0.88</b> ±0.04	<b>0.42</b> ±0.16	0.73±0.01
1d	<b>3.50</b> ±0.86	7.67±0.45	<b>0.55</b> ±0.22	1.53±0.09	<b>0.75</b> ±0.09	0.46±0.09	<b>0.40</b> ±0.09	0.77±0.07
1.5d	<b>3.00</b> ±1.15	5.67±1.75	<b>1.00</b> ±0.19	1.55±0.08	<b>0.89</b> ±0.07	0.62±0.06	<b>0.32</b> ±0.05	0.53±0.04
2d	<b>2.28</b> ±0.80	3.67±0.82	<b>1.00</b> ±0.32	2.67±0.63	0.67±0.17	<b>0.70</b> ±0.09	<b>0.11</b> ±0.03	0.32±0.08
<i>d</i>	<i>varying dimension count</i>							
5	<b>2.28</b> ±0.80	3.67±0.82	<b>1.00</b> ±0.32	2.67±0.63	0.67±0.17	<b>0.70</b> ±0.09	<b>0.11</b> ±0.03	0.32±0.08
7	<b>8.67</b> ±0.56	12.88±0.15	<b>0.72</b> ±0.05	1.07±0.01	<b>0.96</b> ±0.02	0.83±0.01	<b>0.49</b> ±0.01	0.63±0.01
10	<b>19.71</b> ±0.72	30.82±0.98	<b>0.42</b> ±0.13	1.18±0.04	0.70±0.16	<b>0.71</b> ±0.06	<b>0.34</b> ±0.08	0.70±0.02

L-BFGS-B optimizer [58] which can handle parameter bounds out-of-the-box, making it a suitable choice to optimise the augmented Lagrangian<sup>4</sup>. This is made explicit in algs. 1 and 2.

In algs. 1 and 2 we highlight each row (in green) where D-Struct requires edits in the standard NOTEARS-MLP algorithm. Most obvious is the creation of multiple parameters,  $\theta_k$  for each  $k \in [K]$ , where each  $\theta_k$  indicates the set of parameters for one initialisation of NOTEARS-MLP, concerning mostly the architecture in fig. 2. The set  $\{\theta_k : k \in [K]\}$  then denotes the parameters for D-Struct.

From algs. 1 and 2 we learn that information across the different NOTEARS-MLPs is shared in `training_step` (alg. 2). Typically, a training step is solely focused on one structure learner, as is also implied in alg. 1 which iterates over each learner separately. The sharing of information *across* each learner though, is what enforces transportability.

From algs. 1 and 2 we learn that D-Struct hardly increases implementation complexity. In fact, besides architectural alterations (as explained in section 3.1 and fig. 2) it seems that D-Struct requires minimal adjustments in NOTEARS-MLP, as is also the case for other DSFs. This is an important advantage. In fact, Zheng et al. [30] already state the importance of an easy to implement model; they use approximately 60 1ns of code, and we only add an approximate 10 1ns to that. Furthermore, we also noticed a major jump in efficiency where D-Struct drastically reduces computation time. We report computation time in the next section.

## 4 Experiments

Recall from section 3 that D-Struct’s objective is exactly the same as any differentiable structure learner: transform a dataset into a DAG, whilst remaining differentiable. With D-Struct, our aim is to increase performance of any DSF by enforcing transportability on the learner’s outcome structure. As such, the most pressing question is: *does it actually improve existing learners?*

**Transportability.** Before testing accuracy, we first empirically confirm that NOTEARS is not transportable while D-Struct is. We compare NOTEARS with D-Struct with 1000 samples drawn from an Erdos-Renyì (ER) random graph, and split the samples into two equal sized subsets. We evaluate the structural Hamming distance (SHD) between the graphs learned by NOTEARS on each dataset, and the same for the internal graphs learned by D-Struct. The DAGs learnt by D-

<sup>4</sup>While not discussed in previous papers, this also allows to include some prior knowledge on  $\mathcal{I}(\mathbb{P})$ . We discuss this in more detail in appendix E.

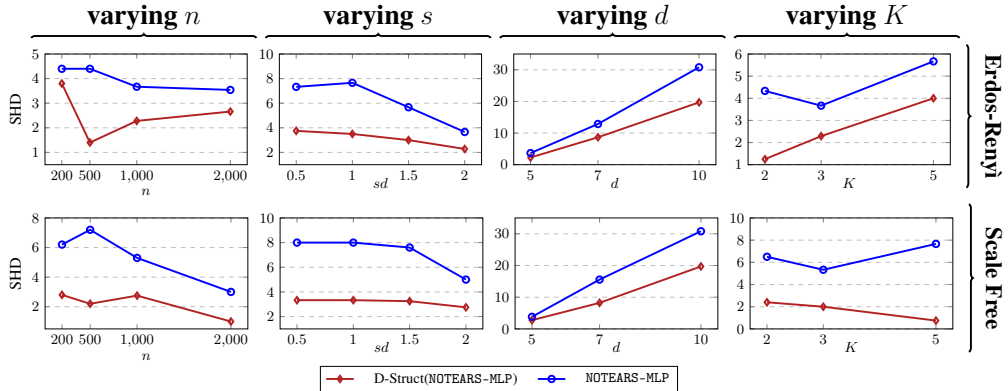


Figure 6: **Empirical results.** We evaluate D-Struct on structure recovery from data. In particular, we report the SHD ( $\downarrow$ ) compared to the true graph. We highlight changes to performance as a function of four different parameters (changing the properties of the task). The results demonstrate that D-Struct outperforms NOTEARS-MLP in all these settings. Additional results are reported in appendix A.

Struct are perfectly transportable (SHD= 0) in 8/10 runs (mean SHD  $0.46 \pm 0.27$ ), with only minor discrepancies in the other cases. Conversely, NOTEARS has a mean SHD of  $1.14 \pm 0.20$ , only displaying transportability in 2 cases. Similar results for other DSFs are reported in appendix A. Next, we evaluate accuracy.

**Accuracy.** The most straightforward way to see if D-Struct is better is to simply repeat the experiments in Zheng et al. [31], and so we have. We report only a subset of our outcomes in the main text, mainly on D-Struct’s improvement over NOTEARS-MLP. However, more metrics and experiments on different DSFs can be found in appendix A. In table 1 we report the false positive rate (FPR), true positive rate (TPR), false discovery rate (FDR), and structural Hamming distance (SHD) of the estimated DAGs using data sampled from different ER random graphs with varying sample size ( $n$ ), expected number of edges ( $s$ ), and dimension count ( $d$ ). In all cases we find that D-Struct significantly improves NOTEARS-MLP (other DSFs in appendix A). A similar conclusion can be drawn from fig. 6, where we report the SHD for more parameters and data from ER as well as Scale Free graphs [30].

**Computational efficiency.** In fig. 5 we learn that despite its parallel ensemble architecture, D-Struct is actually *much* faster than NOTEARS. Note that D-Struct is built *on top* of NOTEARS, meaning this computational gain is not due to differences in implementation. Rather, we believe computation gains are largely due to D-Struct’s parallel learning scheme. Rather than trying to push the entire dataset through one learner, D-Struct splits up the data and learns several small learners rather than one (computationally intensive) learner. Note that this is an important result: the whole reason for having differentiable structure learners is due to their efficiency gains over CIT-based methods.

## 5 Discussion

D-Struct pushes differentiable structure learners forward by introducing transportability to differentiable structure learning, a property that is guaranteed by CIT-based methods. We believe D-Struct will have positive impact on problems depending on structure learners. But there are limitations.

**Limitations.** Pointed out by Kaiser and Sipos [59] and Reisach et al. [60], DSFs are often wrongly used to recover a *causal* DAG. While DAGs are indeed the model of choice to describe causal interactions, there is currently no guarantee that the found DAG can be identified as such. With this we wish to state explicitly that D-Struct’s output is *not* to be interpreted as a causal model.

Of course, as D-Struct learns from observational data, we cannot expect to uncover causal structures without making stricter assumptions. As such, we believe D-Struct is only the first step in the process leading to scientific discovery, functioning as a searchlight if you will. Once D-Struct *suggests* a

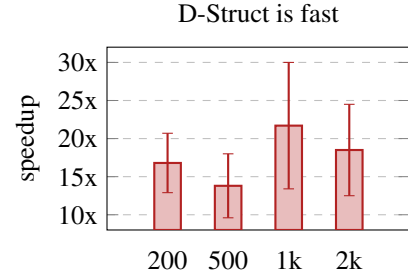


Figure 5: **Efficiency.** Computation time across NOTEARS-MLP and D-Struct, in function of  $n$ . Reported is the speedup of D-Struct over NOTEARS.

link between variables, it is still the scientist’s task to confirm this link in the lab with experimental data. What D-Struct provides then, is a way to reduce the amount of times we have to actually collect experimental data as we now have a more reliable and efficient way to come up with hypotheses.

**Future work.** The inability to uncover causal structure is a consequence of there existing many more useful properties stemming from a CIT-based approach (multiple books concern this very topic [26, 46, 61, 62]). Bridging the gap between these methods is a clear path forward, hopefully increasing these learner’s potential even further.

## Acknowledgments and Disclosure of Funding

This work was funded by: the W.D. Armstrong Trust, The Cystic Fibrosis Trust, The Alan Turing Institute under the EPSRC grant EP/N510129/1 and by the US Office of Naval Research (ONR), NSF 1722516.

## References

- [1] Rohan Bhardwaj, Ankita R Nambiar, and Debojyoti Dutta. A study of machine learning in healthcare. In *2017 IEEE 41st Annual Computer Software and Applications Conference (COMPSAC)*, volume 2, pages 236–241. IEEE, 2017.
- [2] Jeroen Berrevoets, James Jordon, Ioana Bica, Mihaela van der Schaar, et al. Organite: Optimal transplant donor organ offering using an individual treatment effect. *Advances in neural information processing systems*, 33:20037–20050, 2020.
- [3] Mihaela van der Schaar, Ahmed M Alaa, Andres Floto, Alexander Gimson, Stefan Scholtes, Angela Wood, Eoin McKinney, Daniel Jarrett, Pietro Lio, and Ari Ercole. How artificial intelligence and machine learning can help healthcare systems respond to covid-19. *Machine Learning*, 110(1):1–14, 2021.
- [4] Alvin Rajkomar, Jeffrey Dean, and Isaac Kohane. Machine learning in medicine. *New England Journal of Medicine*, 380(14):1347–1358, 2019.
- [5] Jeroen Berrevoets, Ahmed Alaa, Zhaozhi Qian, James Jordon, Alexander ES Gimson, and Mihaela Van Der Schaar. Learning queueing policies for organ transplantation allocation using interpretable counterfactual survival analysis. In *International Conference on Machine Learning*, pages 792–802. PMLR, 2021.
- [6] Susan Athey et al. The impact of machine learning on economics. *The economics of artificial intelligence: An agenda*, pages 507–547, 2018.
- [7] Susan Athey and Guido W Imbens. Machine learning methods that economists should know about. *Annual Review of Economics*, 11:685–725, 2019.
- [8] Sendhil Mullainathan and Jann Spiess. Machine learning: an applied econometric approach. *Journal of Economic Perspectives*, 31(2):87–106, 2017.
- [9] Giuseppe Carleo, Ignacio Cirac, Kyle Cranmer, Laurent Daudet, Maria Schuld, Naftali Tishby, Leslie Vogt-Maranto, and Lenka Zdeborová. Machine learning and the physical sciences. *Reviews of Modern Physics*, 91(4):045002, 2019.
- [10] Alexander Radovic, Mike Williams, David Rousseau, Michael Kagan, Daniele Bonacorsi, Alexander Himmel, Adam Aurisano, Kazuhiro Terao, and Taritree Wongjirad. Machine learning at the energy and intensity frontiers of particle physics. *Nature*, 560(7716):41–48, 2018.
- [11] Sankar Das Sarma, Dong-Ling Deng, and Lu-Ming Duan. Machine learning meets quantum physics. *arXiv preprint arXiv:1903.03516*, 2019.
- [12] George Em Karniadakis, Ioannis G Kevrekidis, Lu Lu, Paris Perdikaris, Sifan Wang, and Liu Yang. Physics-informed machine learning. *Nature Reviews Physics*, 3(6):422–440, 2021.
- [13] Philip G Breen, Christopher N Foley, Tjarda Boekholt, and Simon Portegies Zwart. Newton versus the machine: solving the chaotic three-body problem using deep neural networks. *Monthly Notices of the Royal Astronomical Society*, 494(2):2465–2470, 2020.
- [14] Silviu-Marian Udrescu and Max Tegmark. Ai feynman: A physics-inspired method for symbolic regression. *Science Advances*, 6(16):eaay2631, 2020.

[15] Jan Reinhard Peters. *Machine learning of motor skills for robotics*. University of Southern California, 2007.

[16] Xue Bin Peng, Marcin Andrychowicz, Wojciech Zaremba, and Pieter Abbeel. Sim-to-real transfer of robotic control with dynamics randomization. In *2018 IEEE international conference on robotics and automation (ICRA)*, pages 3803–3810. IEEE, 2018.

[17] Ben Kehoe, Sachin Patil, Pieter Abbeel, and Ken Goldberg. A survey of research on cloud robotics and automation. *IEEE Transactions on automation science and engineering*, 12(2):398–409, 2015.

[18] Pieter Abbeel, Adam Coates, and Andrew Y Ng. Autonomous helicopter aerobatics through apprenticeship learning. *The International Journal of Robotics Research*, 29(13):1608–1639, 2010.

[19] Yanir Kleiman, Simon Pabst, and Patrick Nagle. Boosting vfx production with deep learning. In *ACM SIGGRAPH 2019 Talks*, pages 1–2. 2019.

[20] Dan Ring, Johanna Barbier, Guillaume Gales, Ben Kent, and Sebastian Lutz. Jumping in at the deep end: how to experiment with machine learning in post-production software. In *Proceedings of the 2019 Digital Production Symposium*, pages 1–5, 2019.

[21] Yi Wang. Film and television special effects production based on modern technology: from the perspective of statistical machine learning. In *2022 4th International Conference on Smart Systems and Inventive Technology (ICSSIT)*, pages 833–836. IEEE, 2022.

[22] Alex Davies, Petar Veličković, Lars Buesing, Sam Blackwell, Daniel Zheng, Nenad Tomašev, Richard Tanburn, Peter Battaglia, Charles Blundell, András Juhász, et al. Advancing mathematics by guiding human intuition with ai. *Nature*, 600(7887):70–74, 2021.

[23] John Jumper, Richard Evans, Alexander Pritzel, Tim Green, Michael Figurnov, Olaf Ronneberger, Kathryn Tunyasuvunakool, Russ Bates, Augustin Žídek, Anna Potapenko, et al. Highly accurate protein structure prediction with alphafold. *Nature*, 596(7873):583–589, 2021.

[24] Kathryn Tunyasuvunakool, Jonas Adler, Zachary Wu, Tim Green, Michal Zielinski, Augustin Žídek, Alex Bridgland, Andrew Cowie, Clemens Meyer, Agata Laydon, et al. Highly accurate protein structure prediction for the human proteome. *Nature*, 596(7873):590–596, 2021.

[25] Kiersten M. Ruff and Rohit V. Pappu. Alphafold and implications for intrinsically disordered proteins. *Journal of Molecular Biology*, 433(20):167208, 2021. ISSN 0022-2836. doi: <https://doi.org/10.1016/j.jmb.2021.167208>. URL <https://www.sciencedirect.com/science/article/pii/S0022283621004411>. From Protein Sequence to Structure at Warp Speed: How Alphafold Impacts Biology.

[26] Daphne Koller and Nir Friedman. *Probabilistic graphical models: principles and techniques*. MIT press, 2009.

[27] Sewall Wright. The method of path coefficients. *The annals of mathematical statistics*, 5(3):161–215, 1934.

[28] Max Chickering, Dan Geiger, and David Heckerman. Learning bayesian networks: Search methods and experimental results. In *Proceedings of the fifth international workshop on artificial intelligence and statistics*, 1995.

[29] Jonas Peters, Dominik Janzing, and Bernhard Schölkopf. *Elements of causal inference: foundations and learning algorithms*. The MIT Press, 2017.

[30] Xun Zheng, Bryon Aragam, Pradeep Ravikumar, and Eric P. Xing. DAGs with NO TEARS: Continuous Optimization for Structure Learning. In *Advances in Neural Information Processing Systems*, 2018.

[31] Xun Zheng, Chen Dan, Bryon Aragam, Pradeep Ravikumar, and Eric P. Xing. Learning sparse nonparametric DAGs. In *International Conference on Artificial Intelligence and Statistics*, 2020.

[32] Christopher Meek. Strong completeness and faithfulness in bayesian networks. In *Proceedings of the Eleventh Conference on Uncertainty in Artificial Intelligence*, 1995.

[33] Ann Becker, Dan Geiger, and Christopher Meek. Perfect tree-like markovian distributions. In *Proceedings of the Sixteenth Conference on Uncertainty in Artificial Intelligence*, 2000. URL <https://arxiv.org/abs/1301.3834>.

[34] Monya Baker. 1,500 scientists lift the lid on reproducibility. *Nature*, 533(7604), 2016.

[35] Colin F Camerer, Anna Dreber, Eskil Forsell, Teck-Hua Ho, Jürgen Huber, Magnus Johannesson, Michael Kirchler, Johan Almenberg, Adam Altmejd, Taizan Chan, et al. Evaluating replicability of laboratory experiments in economics. *Science*, 351(6280):1433–1436, 2016.

[36] Robert K Merton. *The sociology of science: Theoretical and empirical investigations*. University of Chicago press, 1973.

[37] Victoria Stodden. The scientific method in practice: Reproducibility in the computational sciences. 2010.

[38] Rohit Bhattacharya, Tushar Nagarajan, Daniel Malinsky, and Ilya Shpitser. Differentiable causal discovery under unmeasured confounding. In *International Conference on Artificial Intelligence and Statistics*, pages 2314–2322. PMLR, 2021.

[39] Trent Kyono, Yao Zhang, and Mihaela van der Schaar. Castle: Regularization via auxiliary causal graph discovery. *Advances in Neural Information Processing Systems*, 33:1501–1512, 2020.

[40] Roxana Pamfil, Nisara Sriwattanaworachai, Shaan Desai, Philip Pilgerstorfer, Konstantinos Georgatzis, Paul Beaumont, and Bryon Aragam. Dynotears: Structure learning from time-series data. In *International Conference on Artificial Intelligence and Statistics*, pages 1595–1605. PMLR, 2020.

[41] Trent Kyono, Yao Zhang, Alexis Bellot, and Mihaela van der Schaar. Miracle: Causally-aware imputation via learning missing data mechanisms. *Advances in Neural Information Processing Systems*, 34, 2021.

[42] Boris van Breugel, Trent Kyono, Jeroen Berrevoets, and Mihaela van der Schaar. Decaf: Generating fair synthetic data using causally-aware generative networks. *Advances in Neural Information Processing Systems*, 34, 2021.

[43] Sébastien Lachapelle, Philippe Brouillard, Tristan Deleu, and Simon Lacoste-Julien. Gradient-based neural dag learning. In *International Conference on Learning Representations*, 2020. URL <https://openreview.net/forum?id=rklbKA4YDS>.

[44] Yue Yu, Tian Gao, Naiyu Yin, and Qiang Ji. Dags with no curl: An efficient dag structure learning approach. In Marina Meila and Tong Zhang, editors, *Proceedings of the 38th International Conference on Machine Learning*, volume 139 of *Proceedings of Machine Learning Research*, pages 12156–12166. PMLR, 18–24 Jul 2021. URL <https://proceedings.mlr.press/v139/yu21a.html>.

[45] Yue Yu, Jie Chen, Tian Gao, and Mo Yu. DAG-GNN: DAG structure learning with graph neural networks. In Kamalika Chaudhuri and Ruslan Salakhutdinov, editors, *Proceedings of the 36th International Conference on Machine Learning*, volume 97 of *Proceedings of Machine Learning Research*, pages 7154–7163. PMLR, 09–15 Jun 2019. URL <https://proceedings.mlr.press/v97/yu19a.html>.

[46] Judea Pearl. *Probabilistic reasoning in intelligent systems: networks of plausible inference*. Morgan kaufmann, 1988.

[47] Martin J Wainwright, Michael I Jordan, et al. Graphical models, exponential families, and variational inference. *Foundations and Trends® in Machine Learning*, 1(1–2):1–305, 2008.

[48] Judea Pearl. Fusion, propagation, and structuring in belief networks. *Artificial intelligence*, 29(3):241–288, 1986.

[49] Judea Pearl. *Causality*. Cambridge university press, 2009.

[50] Thomas Verma and Judea Pearl. Causal networks: Semantics and expressiveness. In *Machine intelligence and pattern recognition*, volume 9, pages 69–76. Elsevier, 1990.

[51] Dan Geiger and Judea Pearl. On the logic of causal models. In *Machine Intelligence and Pattern Recognition*, volume 9, pages 3–14. Elsevier, 1990.

[52] Dan Geiger, Thomas Verma, and Judea Pearl. d-separation: From theorems to algorithms. In *Machine Intelligence and Pattern Recognition*, volume 10, pages 139–148. Elsevier, 1990.

[53] Dan Geiger, Thomas Verma, and Judea Pearl. Identifying independence in bayesian networks. *Networks*, 20(5):507–534, 1990.

- [54] Ronald A Howard and James E Matheson. The principles and applications of decision analysis. *Strategic Decisions Group, Palo Alto, CA*, pages 719–762, 1984.
- [55] JQ Smith. Influence diagrams for statistical modeling. *The Annals of Statistics*, 1, 1989.
- [56] Dan Geiger and Judea Pearl. Logical and algorithmic properties of conditional independence and graphical models. *The annals of statistics*, 21(4):2001–2021, 1993.
- [57] Dimitri P. Bertsekas. *Nonlinear Programming*. Athena Scientific, 3<sup>rd</sup> edition, 2016. ISBN 978-1-886529-05-2.
- [58] Richard H Byrd, Peihuang Lu, Jorge Nocedal, and Ciyou Zhu. A limited memory algorithm for bound constrained optimization. *SIAM Journal on scientific computing*, 16(5):1190–1208, 1995.
- [59] Marcus Kaiser and Maksim Sipos. Unsuitability of NOTEARS for causal graph discovery when dealing with dimensional quantities. *Neural Processing Letters*, pages 1–9, 2022.
- [60] Alexander G Reisach, Christof Seiler, and Sebastian Weichwald. Beware of the simulated dag! varsorability in additive noise models. *arXiv preprint arXiv:2102.13647*, 2021.
- [61] Michael Irwin Jordan. *Learning in graphical models*. MIT press, 1999.
- [62] Steffen L Lauritzen. *Graphical models*, volume 17. Clarendon Press, 1996.
- [63] Ignavier Ng, AmirEmad Ghassami, and Kun Zhang. On the role of sparsity and dag constraints for learning linear dags. In H. Larochelle, M. Ranzato, R. Hadsell, M.F. Balcan, and H. Lin, editors, *Advances in Neural Information Processing Systems*, volume 33, pages 17943–17954. Curran Associates, Inc., 2020. URL <https://proceedings.neurips.cc/paper/2020/file/d04d42cdf14579cd294e5079e0745411-Paper.pdf>.

# Appendix: D-Struct

## Table of Contents

---

<b>A Additional experiments</b>	<b>14</b>
A.1 Settings and details . . . . .	14
A.2 Completed results . . . . .	15
A.3 Other DSFs . . . . .	15
<b>B Causal interpretation</b>	<b>16</b>
<b>C Transportability in non-overlapping domains</b>	<b>17</b>
<b>D Definitions</b>	<b>18</b>
<b>E Incorporating prior knowledge on <math>\mathcal{I}(\mathbb{P})</math> using L-BFGS-B</b>	<b>19</b>

---

## A Additional experiments

Please find our (anonymous) online code repository at:

<https://anonymous.4open.science/r/d-struct-neurips22>

Our code is based on code provided by Zheng et al. [31], and we annotated our code where we used their implementation.

### A.1 Settings and details

In the interest of space, we left out a few details in our main text. Here we discuss hyperparameters (those in addition to the hyperparameters required for the selected DSFs), the evaluation metrics, and how we combine the different parallel DAGs.

**Hyperparameters.** D-Struct inherits hyperparameters from the chosen underlying DSFs. These hyperparameters act in the same way as they would in their original incarnation. For a discussion on these hyperparameters we refer to the relevant literature on these methods specifically.

However, D-Struct also adds two additional parameters:  $K$  and  $\alpha$ . The impact of  $K$  is already discussed in the main text, recapitulated as:  $K$  implicitly determines the sizes of the subsets used to train the parallel DSFs, as such, *for high  $K$  we should have high  $n$* . With both increasing, we report better performance (particularly in Scale-Free DAGs).

The impact of  $\alpha$  is a bit more subtle, and also a function of  $K$ . First, consider fig. 7, displaying the impact on each evaluation metric as a function of different  $\alpha$ . What we find is that setting  $\alpha$  is mostly dependent on  $K$  as lower  $\alpha$  tend to work better with higher  $K$ , and vice versa for lower  $K$ . This makes sense as we sum each  $\mathcal{L}_{\text{MSE}}$ , resulting in a higher value with more  $K$ . If  $\alpha$  is large in a setting with large  $K$ , the regularisation effect would simply be too large. We set our hyperparameters to those which yielded best performance (deduced from fig. 7 for  $\alpha$ , and  $K = 3$  when not varied over as this yielded most stable results overall).

**Evaluation metrics.** The learned graphs from NOTEARS and D-Struct are assessed using four graph metrics namely: (1) Structural Hamming distance (SHD), (2) False discovery rate (FDR), (3) False positive rate (FPR) and (4) True positive rate (TPR). These values are standard when evaluating structure learning methods. We provide some insight into these evaluation metrics below.

*Structural Hamming distance (SHD)* SHD is the total number of edge additions, deletions, and reversals needed to convert the estimated DAG into the true DAG. That means that the

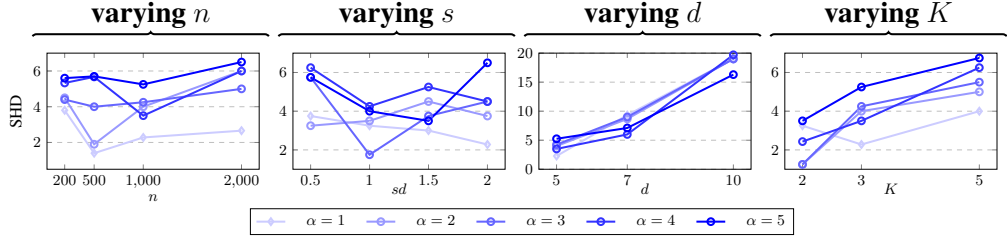


Figure 7: **Results showing the effect of  $\alpha$ .** Depending on the nature of the problem the degree of regularization imposed by  $\alpha$  can vary. This then changes the amount we enforce the similarity between the different D-Struct adjacency matrices.

worst case SHD is  $d^2 - d$ , as we bound the diagonal to be 0 at all times. As such, the reported SHD with varying  $d$  is expected to be higher, not due to hardness of the problem, but as a property of the SHD (see for example fig. 6).

#### False discovery rate (FDR)

Whenever an edge is suggested in the estimated DAG, which is incorrect, we add to the falsely discovered edges. As such, the FDR is defined as the amount of reversed edges and edges that should not exist, divided by the amount of edges in total. Of course, the exception being when no edges are suggested at all (which implies dividing by 0), which naturally has an FDR of zero.

#### False positive rate (FPR)

We sum the edges that should have been reversed and those that should not exist, and divide by the total amount of *non-edges* in the ground truth DAG. A non-edge is an edge that does not exist. With a more connected ground truth DAG, we expect this number to be lower automatically (as the numerator of the FPR would be higher). This is the reason why we let  $s$  be a function of  $d$ , as increasing the amount of expected edges with  $d$  would somewhat counter this effect. Note that, in table 1 we see the FPR increasing proportionate to the factor multiplied with  $d$ , which is as we would expect.

#### True positive rate (TPR)

This signifies the amount of correctly estimated edges, over the amount of edges in the true graph. Note that, reversed edges are counted as wrong edges.

**Combining graphs.** Inference is done by combining the  $K$  internal graphs. In our implementation of D-Struct we combine graphs by averaging the adjacency matrices and apply a threshold to convert the average graph into a binary matrix. The latter is a similar strategy to most DSFs’ strategies to convert a continuous matrix into a binary one. This is a relatively simple method with promising results, in line with what is currently done in literature.

However, given that D-Struct has multiple graphs, we can actually come up with different strategies (a potential topic for future research). Naturally, this would be more relevant with high  $K$ , which in turn requires a larger sample-size, as per our discussion above. Specifically, we enter the domain of ensemble learning. Like D-Struct, ensemble methods need to combine, potentially conflicting, outcomes and provide the user with only one outcome.

One avenue is to not vote on a per-element basis, but on a per-graph basis. Imagine, two graphs in  $K$  that are exactly the same aspire more confidence in their accuracy. We could even relax similarity to an SHD across graphs, where we weight each graph’s “vote” proportionally to their combined SHD. We believe this to be promising area of future research.

## A.2 Completed results

Recall from section 4 that we only reported a subset of the results. In table 4 we report the remainder for NOTEARS-MLP and the D-Struct implementation on scale free graphs.

## A.3 Other DSFs

We repeat the results above for NOTEARS-SOB which is a Sobolev based implementation of NOTEARS, in tables 2 and 3. The main difference here with NOTEARS-MLP is the nonparametric estimation of the

Table 2: **Results on Erdos-Renyi (ER) graphs.** *First block:* We sample five different ER random graphs, and accompanying non-linear structural equations using an index-model. From each system we then sample a varying amount of samples, and evaluate NOTEARS-SOB with D-Struct (indicated as “✓”) and *without* D-Struct (indicated as “✗”). *Second block:* For each row we sample a new ER graph with a varying amount of connectedness ( $s$  indicates the expected amount of edges). *Third block:* For each row we vary the feature dimension count ( $d$ ). *Fourth block:* For each row we vary the number of subsets for D-Struct ( $s$ ). In all cases, we report the average performance in terms of SHD, FPR, TPR, and FDR, with std in scriptsize.

metric	SHD (↓)		FPR (↓)		TPR (↑)		FDR (↓)		
D-Struct	✓	✗	✓	✗	✓	✗	✓	✗	
<i>varying sample size</i>									
<i>varying graph connectedness</i>									
$n$	200	4.80±0.88	1.60±0.09	<b>0.6</b> ±0.16	1.60±0.09	0.49±0.11	0.93±0.01	<b>0.11</b> ±0.03	0.16±0.01
	500	<b>3.20</b> ±0.80	4.60±0.38	<b>2.20</b> ±0.38	4.40±0.40	<b>0.75</b> ±0.09	0.60±0.04	<b>0.27</b> ±0.06	0.44±0.04
	1000	<b>3.20</b> ±0.57	4.00±0.51	<b>1.40</b> ±0.33	3.75±0.52	<b>0.69</b> ±0.07	0.67±0.05	<b>0.19</b> ±0.05	0.38±0.05
$s$	0.5d	<b>12.00</b> ±4.80	39.67±0.31	<b>0.27</b> ±0.13	0.94±0.01	0.67±0.24	0.97±0.03	<b>0.62</b> ±0.20	0.93±0.01
	1d	<b>24.75</b> ±3.35	39.50±0.52	<b>0.61</b> ±0.09	0.99±0.01	<b>0.90</b> ±0.06	0.74±0.09	<b>0.84</b> ±0.02	0.91±0.01
	1.5d	<b>16.00</b> ±3.53	37.78±0.36	<b>0.38</b> ±0.13	0.99±0.01	0.68±0.23	0.73±0.02	0.55±0.18	0.88±0.01
	2d	<b>15.80</b> ±3.00	36.54±0.53	<b>0.33</b> ±0.14	1.04±0.02	<b>0.58</b> ±0.23	0.72±0.07	<b>0.39</b> ±0.16	0.83±0.02
$d$	<i>varying dimension count</i>								
	5	<b>3.20</b> ±0.57	4.00±0.51	<b>1.40</b> ±0.33	3.75±0.52	<b>0.69</b> ±0.07	0.67±0.05	<b>0.19</b> ±0.05	0.38±0.05
	7	<b>5.8</b> ±1.52	14.00±0.87	<b>0.45</b> ±0.15	1.17±0.07	<b>0.84</b> ±0.05	0.611±0.08	<b>0.36</b> ±0.09	0.71±0.05
	10	<b>19.71</b> ±0.72	30.82±0.98	<b>0.42</b> ±0.13	1.18±0.04	0.70±0.16	0.71±0.06	<b>0.34</b> ±0.08	0.70±0.02
$K$	<i>varying subset count</i>								
	2	4.00±0.46	3.67±0.57	<b>2.75</b> ±0.31	3.67±0.57	0.64±0.06	0.70±0.06	<b>0.33</b> ±0.04	0.36±0.06
	3	<b>3.20</b> ±0.57	4.00±0.51	<b>1.40</b> ±0.33	3.75±0.52	<b>0.69</b> ±0.07	0.67±0.05	<b>0.19</b> ±0.05	0.38±0.05
	5	<b>2.60</b> ±0.16	3.75±0.41	<b>1.40</b> ±0.16	3.75±0.41	<b>0.78</b> ±0.02	0.67±0.04	<b>0.16</b> ±0.02	0.38±0.05

structural equations in  $\hat{\mathcal{G}}$ . Note that, future implementations of DSFs broadly alter the way in which the structural equations are estimated, and much less on how the proposed structure is evaluated to be a DAG (as they are mostly based on eq. (3)). Overall, we find that NOTEARS-SOB behaves the same as NOTEARS-MLP: D-Struct vastly improves performance.

Note that code to reproduce above results is provided in the online code repository linked to above.

## B Causal interpretation

Causal relationships between variables are often expressed as DAGs [49]. While D-Struct is able to recover DAGs more reliably, there is actually no guarantee that the found DAG can be interpreted as a causal DAG. There is a simple reason for this: we do not make any additional identification assumptions on the structural equations when learning DAGs, at least not beyond what is already assumed in the used DSFs. Furthermore, should D-Struct be combined with a DSF that *is* able to recover a causal DAG<sup>5</sup>, the way in which the  $K$  internal DAGs are combined may violate these assumptions (recall DAG combination from appendix A.1).

With D-Struct, we recover a Bayesian network (BN), which is directed, yet the included directions are not necessarily meaningful. The only guarantee we have with BNs is that they resemble a distribution, which express some conditional distributions (as per the independence sets in section 2.1). Order is not accounted for in these independence sets. For more information regarding this, we refer to appendix D and Koller and Friedman [26].

However, as is indicated in Koller and Friedman [26, Chapter 21], a “good” BN structure should correspond to causality, where edges  $X \rightarrow Y$  indicated that  $X$  causes  $Y$ . Koller and Friedman [26] state that BNs with a causal structure tend to be sparser. Though, if queries remain probabilistic, it doesn’t matter whether or not the structure is causal, the answers will remain the same. Only when

<sup>5</sup>We know of none that is able to.

Table 3: **Results on Scale-Free (SF) graphs.** *First block:* We sample five different SF random graphs, and accompanying non-linear structural equations using an index-model. From each system we then sample a varying amount of samples, and evaluate NOTEARS-SOB with D-Struct (indicated as “✓”) and *without* D-Struct (indicated as “✗”). *Second block:* For each row we sample a new SF graph with a varying amount of connectedness ( $s$  indicates the expected amount of edges). *Third block:* For each row we vary the feature dimension count ( $d$ ). *Fourth block:* For each row we vary the number of subsets for D-Struct ( $s$ ). In all cases, we report the average performance in terms of SHD, FPR, TPR, and FDR, with std in scriptsize.

metric	SHD (↓)		FPR (↓)		TPR (↑)		FDR (↓)	
D-Struct	✓	✗	✓	✗	✓	✗	✓	✗
<i>varying sample size</i>								
200	6.00±0.69	3.8±0.25	1.8±0.20	1.27±0.08	0.49±0.12	0.83±0.03	0.63±0.08	0.39±0.02
500	<b>3.40</b> ±0.88	4.60±0.25	<b>0.67</b> ±0.14	1.53±0.08	0.57±0.09	0.69±0.03	<b>0.41</b> ±0.12	0.48±0.03
1000	<b>2.75</b> ±0.86	4.33±0.50	<b>0.58</b> ±0.22	1.44±0.17	0.61±0.15	0.76±0.05	<b>0.36</b> ±0.15	0.44±0.05
<i>varying graph connectedness</i>								
0.5d	<b>14.11</b> ±5.40	39.53±0.37	<b>0.31</b> ±0.13	0.89±0.01	<b>0.22</b> ±0.14	0.20±0.11	<b>0.42</b> ±0.17	0.93±0.01
1d	<b>8.11</b> ±3.96	39.46±0.38	<b>0.13</b> ±0.09	0.89±0.01	<b>0.00</b> ±0.00	0.16±0.09	<b>0.22</b> ±0.15	0.99±0.01
1.5d	<b>15.20</b> ±3.44	38.31±0.41	<b>0.32</b> ±0.14	1.05±0.01	<b>0.58</b> ±0.23	0.52±0.07	<b>0.40</b> ±0.17	0.98±0.01
2d	<b>15.20</b> ±3.44	38.25±0.44	<b>0.32</b> ±0.14	1.04±0.01	<b>0.58</b> ±0.23	0.50±0.07	<b>0.40</b> ±0.17	0.89±0.01
<i>varying dimension count</i>								
5	<b>2.75</b> ±0.86	4.33±0.50	<b>0.58</b> ±0.22	1.44±0.17	0.61±0.15	0.76±0.05	<b>0.36</b> ±0.15	0.44±0.05
7	<b>8.25</b> ±3.09	15.00±0.22	<b>0.55</b> ±0.21	1.00±0.01	<b>0.96</b> ±0.08	0.78±0.02	<b>0.49</b> ±0.16	0.76±0.01
10	<b>16.80</b> ±4.21	35.75±0.33	<b>0.36</b> ±0.17	0.99±0.01	0.58±0.24	0.67±0.03	<b>0.42</b> ±0.17	0.85±0.01
<i>varying subset count</i>								
2	<b>3.00</b> ±0.42	6.00±0.30	<b>0.53</b> ±0.21	2.00±0.10	<b>0.66</b> ±0.04	0.57±0.04	<b>0.21</b> ±0.07	0.60±0.03
3	<b>2.75</b> ±0.86	4.33±0.5	<b>0.58</b> ±0.22	1.44±0.17	0.61±0.15	0.76±0.05	<b>0.36</b> ±0.15	0.44±0.05
5	<b>2.80</b> ±0.57	5.25±0.21	<b>0.73</b> ±0.15	1.75±0.07	<b>0.74</b> ±0.09	0.68±0.03	<b>0.31</b> ±0.07	0.53±0.02

we are interested in interventional queries (by using do-calculus) we have to make sure the DAG is a causal one.

The above is a pragmatic view. To our knowledge, there is no real proof stating that sparser DAGs are (even more likely to be) causal. However, it could offer guidance to try and recover a causal DAG, assuming it to be sparse [63].

## C Transportability in non-overlapping domains

Consider the multi-origin setting, where we have at least two datasets, each stemming from a different source. It is entirely possible that, given the different sources, these datasets are not comparable in terms of recorded features. We can recognise two major manifestations of this phenomenon: either (i) the supports of the datasets do not match, or (ii) the dimensions do not match.

**(i) Different support.** Recall from section 2.1 that DAGs encode a set of independence statements. As such, it is mainly independence that governs structure. Transportability in the setting of conflicting support, thus requires some (mild) assumptions. Specifically, we require that independence holds, regardless of support. This is mostly a pragmatic assumption. If for example, we find that  $\mathcal{X}_i \perp\!\!\!\perp \mathcal{X}_j$ , where each component denotes a dimension in  $\mathcal{X}$ , we usually don’t specify over what support this independence holds. Implicitly, we assume that independence holds, regardless of what area in  $\{\mathcal{X}_i, \mathcal{X}_j\}$  we find ourselves in.

Note that the chosen distributions in  $\mathcal{P}$  in section 3.2 govern the entire domain  $[N]$ , and as a consequence  $\mathcal{X}$ . As such, the problem of conflicting support does not manifest in our solution of single-origin D-Struct. In case one chooses distributions that do not cover  $[N]$  equally, we have to assume independence is constant across different supports (i.e. the assumption explained above).

**(ii) Different dimensions.** A more difficult setting of conflicting domains, is when we record different variables in each of the multi-origin datasets. In order for a DAG to be transportable, we *require* the

Table 4: **Results on Scale-Free (SF) graphs.** *First block:* We sample five different SF random graphs, and accompanying non-linear structural equations using an index-model. From each system we then sample a varying amount of samples, and evaluate NOTEARS-MLP with D-Struct (indicated as “✓”) and *without* D-Struct (indicated as “✗”). *Second block:* For each row we sample a new SF graph with a varying amount of connectedness ( $s$  indicates the expected amount of edges). *Third block:* For each row we vary the feature dimension count ( $d$ ). *Fourth block:* For each row we vary the number of subsets for D-Struct ( $s$ ). In all cases, we report the average performance in terms of SHD, FPR, TPR, and FDR, with std in scriptsize.

metric	SHD (↓)		FPR (↓)		TPR (↑)		FDR (↓)	
D-Struct	✓	✗	✓	✗	✓	✗	✓	✗
<i>varying sample size</i>								
200	<b>2.80</b> ±0.86	6.20±0.57	<b>0.73</b> ±0.28	2.07±0.19	<b>0.80</b> ±0.11	0.54±0.08	<b>0.26</b> ±0.11	0.62±0.06
500	<b>2.20</b> ±0.80	7.20±0.66	<b>0.27</b> ±0.12	2.20±0.18	<b>0.77</b> ±0.13	0.37±0.09	<b>0.14</b> ±0.06	0.72±0.06
1000	<b>3.25</b> ±1.49	5.33±0.61	<b>0.75</b> ±0.43	1.78±0.20	<b>0.68</b> ±0.15	0.66±0.08	<b>0.29</b> ±0.18	0.53±0.06
<i>varying graph connectedness</i>								
0.5d	<b>3.33</b> ±0.88	8.00±0.37	<b>0.50</b> ±0.19	1.17±0.06	<b>0.92</b> ±0.08	0.38±0.05	<b>0.41</b> ±0.08	0.82±0.03
1d	<b>3.33</b> ±0.89	8.00±1.00	<b>0.50</b> ±0.19	1.17±0.17	<b>0.92</b> ±0.08	0.38±0.13	<b>0.41</b> ±0.08	0.82±0.07
1.5d	<b>3.25</b> ±0.41	7.67±0.31	<b>0.50</b> ±0.07	1.17±0.04	<b>0.94</b> ±0.04	0.42±0.06	<b>0.43</b> ±0.03	0.80±0.03
2d	<b>2.75</b> ±1.03	5.00±1.00	<b>0.33</b> ±0.23	1.22±0.22	<b>0.64</b> ±0.15	0.50±0.07	<b>0.14</b> ±0.09	0.48±0.12
<i>varying dimension count</i>								
5	<b>3.25</b> ±1.49	5.33±0.61	<b>0.75</b> ±0.43	1.78±0.20	<b>0.68</b> ±0.15	0.66±0.08	<b>0.29</b> ±0.18	0.53±0.06
7	<b>8.22</b> ±1.31	15.67±0.14	<b>0.54</b> ±0.09	1.04±0.01	<b>0.98</b> ±0.02	0.83±0.03	<b>0.54</b> ±0.04	0.76±0.01
10	<b>16.80</b> ±4.21	35.75±0.33	<b>0.36</b> ±0.17	0.99±0.01	<b>0.58</b> ±0.24	0.67±0.03	<b>0.42</b> ±0.17	0.85±0.01
<i>varying subset count</i>								
2	<b>2.40</b> ±0.24	6.50±0.46	<b>0.53</b> ±0.08	2.16±0.15	<b>0.83</b> ±0.05	0.50±0.06	<b>0.21</b> ±0.03	0.65±0.06
3	<b>2.00</b> ±1.04	5.33±0.6	<b>0.33</b> ±0.47	1.78±0.20	<b>0.68</b> ±0.14	0.66±0.09	<b>0.14</b> ±0.09	0.53±0.06
5	<b>0.75</b> ±0.48	5.25±0.21	<b>0.25</b> ±0.16	2.55±0.11	<b>1.00</b> ±0.00	0.33±0.05	<b>0.09</b> ±0.05	0.76±0.03

variable sets to correspond. As such, we are only able to work with overlapping intersections of the non-overlapping domains. Doing so requires some additional assumptions on the noise: assuming we record some noise on each variable, we have to make the additional assumption that the noise is independent of the other variables, or at least the variables outside the intersection between domains. The latter is made quite often, and should not limit applicability of D-Struct in this setting too much (recall that applicability of D-Struct is mostly determined by the used DSF). The reason relates to the second assumption, below.

The second assumption is a bit stricter: any variables outside the intersection cannot be confounding variables inside the intersection. If two variables have no direct edges, and the nodes part of an indirect edge fall outside the domain-intersection, we have to expect the DSF to find an edge between these two nodes. While this direct edge is wrong, this is actually expected behaviour of most DSFs as the algorithms will find these variables to be correlated (due to the third, now unobserved, variable). The only way to overcome these situations, is to use DSFs that naturally handle unobserved confounding.

## D Definitions

**Definition 3** (Markov blanket.). *A Markov blanket of a random variable  $X_i$  in a random set  $\mathcal{X} := \{X_1, \dots, X_d\}$  is any subset  $\mathcal{X}' \subset \mathcal{X}$  where, when conditioned upon, results in independence between  $\mathcal{X} \setminus \mathcal{X}'$  (the other variables) and  $X_i$ ,*

$$X_i \perp\!\!\!\perp \mathcal{X} \setminus \mathcal{X}' | \mathcal{X}'. \quad (6)$$

We will denote the Markov blanket of  $X_i$  as  $\mathcal{X}'(X_i)$ .

In principle, def. 3 means that  $\mathcal{X}'$  contains all the information present in  $\mathcal{X}$  to infer  $X_1$ . Note that this does not mean that  $\mathcal{X} \setminus \mathcal{X}'$  contains *no* information to infer  $X_1$ , but variables in  $\mathcal{X}'$  are sufficient to predict  $X_1$ .

One step further, is a *Markov boundary* [46]:

**Definition 4** (Markov boundary.). A Markov boundary of a random variable  $X_i$  of a random set  $\mathcal{X} := \{X_1, \dots, X_d\}$  is any subset  $\mathcal{X}^- \subset \mathcal{X}$  which is a Markov blanket (def. 3) itself, but does not contain any proper subset which itself is a Markov blanket. We will denote the Markov boundary of  $X_i$  as  $\mathcal{X}^-(X_i)$ .

We can relate the Markov boundary (def. 4) to probabilistic graphical modelling, as from a simplified factorisation (in eq. (1)), we can compose a Bayesian network. Specifically, each variable  $X_j \in \mathcal{X}^-(X_i)$  depict one of three types of relationships:  $X_j$  is a parent of  $X_i$ , denoted as  $\text{Pa}(X_i) = X_j$ ;  $X_j$  is a child of  $X_i$ , denoted as  $\text{Ch}(X_i) = X_j$ ; or  $X_j$  is a parent of a child of  $X_i$ , denoted as  $\text{Pa}(\text{Ch}(X_i)) = X_j$ . Assuming that  $\mathbb{P}_{\mathcal{X}}$  is governed by a Markov random field (rather than a Bayesian network) simplifies things, as the Markov boundary depicts only directly connected variables.

While the above may suggest that the Markov boundary only implies a vague graphical structure, doing this for ever variable in  $\mathcal{X}$  will strongly constraint the possible graphical structures respecting any found independence statements. D-separation (def. 1) is then used to further limit the set of potential DAGs [29, 49]. Relating above definitions to those discussed in section 2.1. For more information regarding the above, we refer to Koller and Friedman [26].

## E Incorporating prior knowledge on $\mathcal{I}(\mathbb{P})$ using L-BFGS-B

Consider the following, where we wish to discover a structure between 3 variables:  $X, Y, Z$ , where the ground truth satisfies  $X \perp\!\!\!\perp Y | Z$ . According to the rules of  $d$ -peration (cfr. def. 1), we are always in a structure where  $X$  and  $Y$  are *only* directly connected to  $Z$ , i.e. no direct connection between  $X$  and  $Y$  exists. Let us further assume that the system is linear (as this is what vanilla NOTEARS assumes, but without loss of generality towards recent NOTEARS extensions), then we have the following,

structural equations	structure	adjacency matrix
$X := \epsilon_X,$ $Z := \beta_{Z,X}X + \epsilon_Z,$ $Y := \beta_{Y,Z}Z + \epsilon_Y,$	$(X) \rightarrow (Z) \rightarrow (Y)$	$A = \begin{pmatrix} 0 & 0 & 1 \\ 0 & 0 & 0 \\ 0 & 1 & 0 \end{pmatrix}.$

Naturally, using only conditional independence, the direction of the arrows are not identifiable as explained above. However, NOTEARS is unable to narrow it down to the equivalence classes expressed in def. 1. The reason is simple, NOTEARS' three optimisation components (the  $h$ -measure, an  $L_2$  loss, and an  $L_1$  regularizer on  $A$ , [63]) are satisfied exactly the same with the following system:

structural equations	structure	adjacency matrix
$X := \epsilon_X,$ $Z := \beta_{Z,X}X + \epsilon_Z,$ $Y := \beta_{Y,X}X + \epsilon'_Y,$	$(X) \rightarrow (Z) \rightarrow (Y)$	$A' = \begin{pmatrix} 0 & 1 & 1 \\ 0 & 0 & 0 \\ 0 & 0 & 0 \end{pmatrix},$

where  $\beta_{Y,X} = \beta_{Y,Z}\beta_{Z,X}$ , and  $\epsilon'_Y = \beta_{Y,Z}\epsilon_Z + \epsilon_Y$  resulting in  $Y$  being determined again by a simple linear equation. Both systems allow the same data to be generated, however under the constraint that  $X \perp\!\!\!\perp Y | Z$  only the former is possible.

We argue that NOTEARS (and extensions) are unable to differentiate between them. Consider the components optimised by NOTEARS: both solutions propose a DAG (i.e.  $h(A) = h(A') = 0$ ); each DAG has an equal amount of arrows, leading to the same  $L_1$ -loss across  $A$  and  $A'$ ; and each equation is linear so NOTEARS is able to perfectly converge to each solution using its  $L_2$  loss. Given that each component scores exactly the same, NOTEARS is unable to differentiate between these two results. Crucially however, in the latter system  $X$  is *always* dependent of  $Y$ , resulting in  $X \not\perp\!\!\!\perp Y | Z$  (and even  $X \not\perp\!\!\!\perp Y$  eliminating v-structures) which is completely opposite to the former system.

**Prior Markov independencies.** We can however force known independence statements into DSFs a priori, using the L-BFGS-B optimizer. For example, consider the following  $I = X_i \perp\!\!\!\perp X_j | Z$ . If  $I$  is known a priori, then we also know there cannot (under any circumstance) exist a direct link

between  $X_i$  and  $X_j$  as this would immediately contradict  $I$  which in turn would invalidate a structure proposing such a link.

As such, we propose to fix these directed edges to  $0 \rightarrow \mathcal{A}_{ij}(\mathcal{G}), \mathcal{A}_{ji}(\mathcal{G})$ , and exclude them from gradient calculation. This will not only constraint each DSL in step 2 above resulting in easier convergence, but it will also enforce any known  $\mathcal{I}(\mathbb{P}_{\mathcal{X}})$  to be taken into account. Setting  $A_{X,Y} = A_{Y,X} = 0$  would immediately restrict NOTEARS from converging to this false solution as the solution would require  $A_{X,Y}$  to be 1. The same approach is currently used in NOTEARS (and consequentially D-Structs parallel DSFs), by setting bounds of each diagonal element in  $A$  to  $(0, 0)$ .

Setting some elements to 0 using the L-BFGS-B bounds, we effectively limit the set of possible solutions. In fact, when applied to the above problems, the second solution would sit *outside* the set of possible solutions, ensuring that NOTEARS cannot converge to it.